Dynamic-Multiple Model for Agricultural Ecosystem Evolution and Effects of Biological Interventions

Qihong Wu *, #, Zihan Mei #, Zhuoran Zhang #

School of Electrical Engineering, Chongqing University, Chongqing, China, 400044

* Corresponding Author Email: cquwqh@stu.cqu.edu.cn

*These authors contributed equally.

Abstract. As forest resources are continuously converted into agricultural land, the ecosystem balance faces significant challenges, disrupting local biodiversity. To understand the evolutionary process of agricultural ecosystems, a Dynamic-Multiple (DM) agricultural ecosystem model is proposed. The Lotka-Volterra model is referenced, integrating natural processes and human decision-making, to develop the DM model and examine the population biomass variations of four species in the eastern Hubei Yangtze Plain. Biomass variation trends of different species under the influence of five factors are identified. The DM agricultural ecosystem is modified by introducing two new species, snakes and mice. Re-analysis of biomass variations shows that the introduction of snakes and mice significantly impacts bat biomass, with no notable effect on other species. The model is further modified by incorporating Plant Growth-Promoting Bacteria (PGPB) and pollination effects. PGPB is found to primarily influence crop biomass, while the pollination effect mainly affects crop growth rate. When herbicides are removed during sowing in the third year, a significant decline in crop biomass is observed, and the number of consumers tends to stabilize. The model is validated through the above three cases.

Keywords: Agricultural Ecosystems, Lotka-Volterra Model, Dynamic-Multiple Model.

1. Introduction

In recent years, driven by the combined pressures of global population growth and increasing agricultural demand, land-use patterns have undergone significant transformation. Critical natural ecosystems, including forests and wetlands, are being rapidly converted into agricultural land at an alarming rate. This trend is evident across multiple regions worldwide, with both its scale and pace continuing to expand at an accelerating rate [1]. This change fractures complex ecological networks, undermining biodiversity, perturbing biogeochemical cycles, and eroding the inherent resilience of ecosystems [2]. Although agricultural expansion has underpinned global food security, it has simultaneously precipitated ripple effects across species interactions—disrupting predator—prey relationships, reshaping competitive hierarchies, and weakening mutualisms. A deeper mechanistic understanding of how these interlinked processes regulate the stability and functioning of agroecosystems is therefore essential to inform land-use strategies that reconcile high productivity with long-term ecological integrity [3].

Early ecosystem models—exemplified by the Lotka–Volterra framework—have yielded critical insights into predator–prey and competitive interactions [4]. Nonetheless, these formulations typically fail to capture the dynamic interplay between intrinsic ecological processes and management decisions that define agroecosystems [5]. Recent efforts have begun to bridge this gap by embedding harvest periodicity and chemical controls [6] into population-dynamics models. Yet, integrated treatments that concurrently encompass multispecies interactions, biological invasions, and microbial-mediated functions—such as those conferred by plant growth–promoting bacteria (PGPB)—remain scarce in the literature [7].

Anthropogenic activities exert profound influences on ecological dynamics [8]. For instance, pesticide applications have been demonstrated to destabilize predator—prey equilibria, frequently precipitating pest outbreaks [9], while episodic crop harvests generate resource pulses that reshape consumer population trajectories [10]. Furthermore, the contribution of microbial symbionts—such

as plant growth–promoting bacteria—to crop vigor and stress tolerance has garnered increasing attention [11], yet their integration into multispecies modeling frameworks remains limited. Likewise, pollination services—vital for approximately 75% of global food crops—are routinely represented in oversimplified terms, despite mounting evidence for their dual role in bolstering both plant diversity and yield [12]

The Dynamic-Multiple (DM) agricultural ecosystem model presented in this article integrates the Lotka–Volterra framework with anthropogenic decision rules to simulate species biomass trajectories across a suite of environmental and management regimes. In contrast to conventional approaches, the DM model explicitly incorporates: (1) seasonal fluctuations in environmental carrying capacity; (2) trophic effects arising from species reintroductions (e.g., snakes, mice); (3) synergistic plant–microbe and pollination interactions mediated by PGPB and chiropteran visitors; and (4) ecological outcomes following reductions in chemical inputs (e.g., herbicide withdrawal). Deployment of this model within the Eastern Hubei Yangtze Plain—a landscape typified by intensive cultivation and simplified food-web architectures—facilitates: (i) quantification of biotic–abiotic feedbacks governing population stability; (ii) evaluation of cascading, top-down trophic controls; and (iii) appraisal of the capacity of biological interventions to bolster agroecosystem resilience.

2. Establish of Dynamic-Multiple (DM)Agricultural Ecosystem Model

Conversion of forests to agricultural land has become pervasive worldwide, profoundly altering the structure and function of previously intact ecosystems. Accurate ecosystem models are therefore essential for elucidating and forecasting species dynamics, preserving ecological balance, and guiding sustainable agricultural development amid this land-use transition. Hence, a Dynamic–Multiple (DM) agricultural ecosystem model is presented that integrates both natural processes and human decision-making. Mechanistic analyses reveal how these coupled factors drive ecosystem behavior, offering insights into the interplay between anthropogenic activities and ecosystem resilience.

2.1. The Development of a Basic Ecosystem Framework

The overall basic ecosystem framework is illustrated in Figure 1.

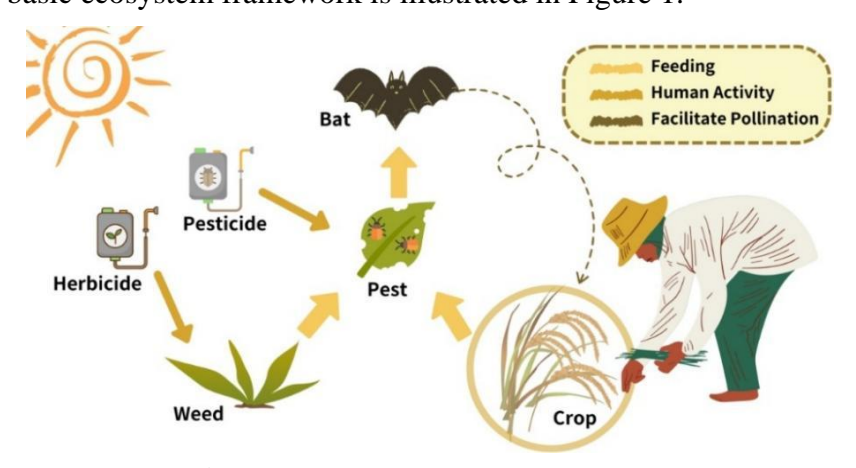


Figure 1. Basic ecosystem framework

Crops and weeds, as primary producers, engage in competitive interactions that are well captured by the Lotka–Volterra framework. For each species iii (crop or weed), the population dynamics under interspecific competition are given by:

$$\frac{dP_i}{dt} = r_{P_i} \cdot P_i \left(1 - \frac{P_i + d_{ji} \cdot P_j}{K_{P_i}} \right) \tag{1}$$

Where P_i represents the number of plants of a single-species; r_{Pi} is the intrinsic growth rate of this species; K_{Pi} is the maximum environmental carrying capacity of this species, that is, the maximum

number that the population of this species can stably reach when resources in the environment are limited; d_{ji} is the competition coefficient, indicating the degree of influence of the competitor on the population of this species. The larger d_{ji} is, the stronger the inhibitory effect of the competitor on the growth of this species; P_j is the population number of the competitor.

Consumer communities exhibit classic predator—prey interactions. For a single prey species i subject to predation by a consumer predator j, the prey and consumer dynamics are expressed as:

$$\frac{dC_{pi}}{dt} = r_{C_{pi}} \cdot C_{pi} \left(1 - \frac{C_{pi}}{K_{C_{p}i}} \right) - f_{ji} \cdot C_{pi}$$

$$\tag{2}$$

$$\frac{dC_{pj}}{dt} = r_{C_{pj}} \cdot C_{pj} \left(1 - \frac{C_{pj}}{K_{C_{pj}}} \right) + g_j \cdot f_{ji} \cdot C_{pj}$$

$$\tag{3}$$

Where C_{pi} represents the number of a certain prey species in the predator; C_{pj} denotes the number of a certain prey species in the prey; r_{Cpi} is the growth rate of the prey in the predator; r_{Cpj} is the growth rate of the prey in the prey; K_{Cpi} is the maximum environmental carrying capacity of the predator; K_c is the maximum environmental carrying capacity of the prey. f_{ji} is the capture efficiency of the predator on the prey species; g_i is the effect of the growth rate on the prey.

Consumer impacts on producer abundance are negligible given their relative densities; however, insect herbivory still imposes direct damage on crop biomass. Accordingly, the instantaneous rate of crop damage (*DPC*) is defined as:

$$DPC = \gamma_D \cdot C_{ni} \cdot P_i \tag{4}$$

Where γ_D is the damage coefficient of insects to crops.

In actual agricultural production, herbicides are commonly used to control the growth of weeds, while pesticides are commonly used to control the damage caused by insects. The temporal inhibitory effect of herbicide on weed and insect biomass is defined as:

$$PE = \gamma_P \cdot P_i \tag{5}$$

$$CE = \gamma_C \cdot C_i \tag{6}$$

Where PE and CE denote the effect on weed and insect, respectively; γ_P represents the control coefficient of herbicides on weeds; γ_C is the control coefficient of pesticides on insects.

Crop harvest represents a critical component of agricultural practice with significant ecosystem ramifications. The variable *HAR* quantifies the reduction in crop density due to harvesting over time. Because harvesting is confined to a brief autumnal window each year, *HAR* is naturally periodic and may be expressed as:

$$HAR = \begin{cases} p_{\text{harvest}} \cdot P_i, & \text{if } t \in [t_{\text{start}}, t_{\text{end}}] \\ 0, & \text{otherwise} \end{cases}$$
 (7)

Where p_{harvest} is the harvest rate of crops; t_{start} and t_{end} denote the start and the end of the harvest period in the reference year;

Crop harvest season often coincides with a transient surge in pest abundance, which in turn drives a short-term increase in secondary consumer (predator) numbers via classic predator—prey coupling. To capture this effect, the variable *CHAR* is introduced to quantify the periodic consumer response to harvesting:

$$CHAR_{i} = \begin{cases} c_{\text{harvest}} \cdot C_{i}, & \text{if } t \in [t_{\text{start}}, t_{\text{end}}] \\ 0, & \text{otherwise} \end{cases}$$
 (8)

Where Charvest represents the growth rate of each consumer species during harvest.

Seasonal variation in environmental carrying capacity exerts a profound influence on population dynamics. As summer progresses, rising temperatures and enhanced resource availability elevate the maximum carrying capacity, whereas cooler winter conditions induce a decline. To capture this periodicity at monthly resolution, the carrying capacity $K_i(t)$ is modeled as a sinusoidal function:

$$K_{i}(t) = K_{i0} \left(1 + \alpha \cdot \sin \left(\frac{\pi}{6} \cdot t \right) \right) \tag{9}$$

Where K_{i0} represents the basic maximum environmental carrying capacity of the species; α indicates the degree of seasonal variation in the maximum environmental carrying capacity of the species.

The inhibitory impact of predator-mediated trophic transfer of toxins can be captured by a pollutant-dependent reduction in intrinsic growth rate. The effective growth rate r_i is illustrated as:

$$r_i = r_{i0} \cdot e^{-\delta t} \tag{10}$$

Where r_{io} is the basic growth rate of the species, and δ is the environmental pollution factor associated with harmful substances, which decreases the growth rate of the species over time.

Based on the preceding analysis, a comprehensive model integrating producers, consumers(prey), consumers(predators) can be derived as (11), (12), (13):

$$\frac{dP_i}{dt} = r_i \cdot P_i \left(1 - \frac{P_i + d_{ji} \cdot P_j}{K_{pi}} \right) - DPC - PE - HAR$$
(11)

$$\frac{dC_{pi}}{dt} = r_{C_{pi}} \cdot C_{pi} \left(1 - \frac{C_{pi}}{K_{C_{pi}}} \right) - f_{ji} \cdot C_{pi} \cdot C_{pj} - CE + CHAR_i$$

$$(12)$$

$$\frac{dC_{pj}}{dt} = r_{C_{pi}} \cdot C_{pj} \left(1 - \frac{C_{pj}}{K_{C_{pi}}} \right) + g_j \cdot f_{ji} \cdot C_{pj} \cdot C_{pi} + CHAR_i$$

$$\tag{13}$$

2.2. Improvement of DM Agricultural Ecosystem

Over time, plant and animal communities in edge habitats undergo gradual development and restoration. As vegetation rejuvenates and environmental conditions improve, these areas become increasingly hospitable to native species. In the second year of the modeled successional phase—based on the original prototype—snakes and mice were introduced, and their effects on the nascent ecosystem were assessed through simulation. The improved ecosystem is illustrated in Figure 2.

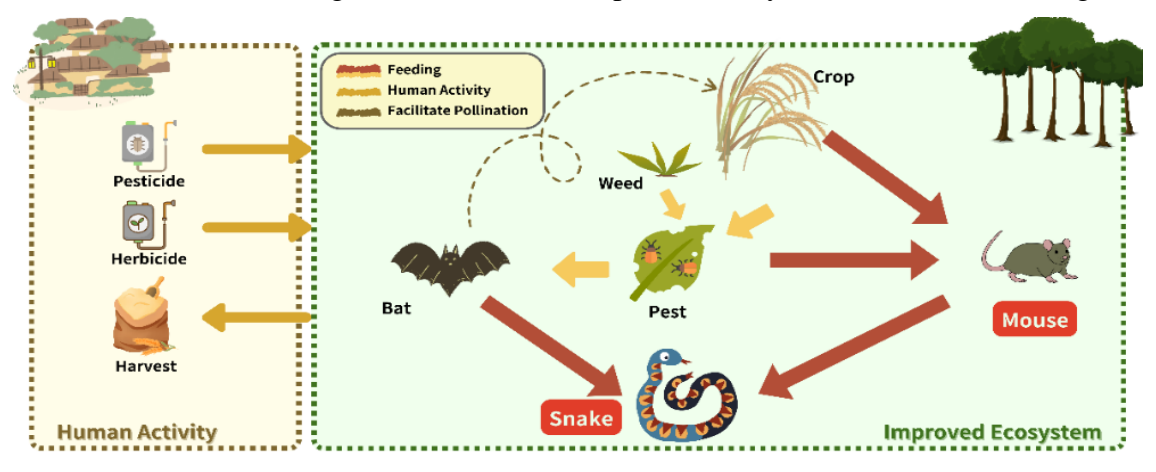


Figure 2. Improved ecosystem framework

In the refined model, bats subsume the ecological roles of both bats and birds. Mice function as secondary consumers, feeding on crops and pests without competing with bats due to ample resources, while snakes, as tertiary consumers, prey upon both mice and bats.

Decomposers mineralize organic matter into inorganic compounds, which are re-assimilated by plants, thereby driving nutrient cycling and reinforcing ecosystem stability. In addition to their predatory role, bats act as nocturnal pollinators, dispersing pollen and enhancing plant propagation; accordingly, the revised model incorporates both plant growth–promoting bacteria (PGPB) and bat pollination efficiency.

PGPB growth is assumed to follow a logistic model, described by:

$$\frac{dG}{dt} = r_G \cdot G \left(1 - \frac{G}{K_G} \right) \tag{14}$$

Where G denotes the colony density of PGPB; r_G denotes the growth rate of PGPB; K_G indicates the maximum environmental carrying capacity of PGPB.

PGPB synthesize phytohormones, stimulating root development and improving crop vigour; their net effect on crop growth rate is denoted r_{PGPB} :

$$r_{\text{PGPB}} = \gamma_{\text{PGPB1}} \cdot G \tag{15}$$

Where γ_{PGPB1} denotes the influence factor of PGPB with respect to the growth rate of crops.

PGPB enhance soil structure through organic-matter decomposition and suppress phytopathogens, thereby increasing crop disease resistance and elevating the maximum environmental carrying capacity, denoted K_{PGPB} :

$$K_{\text{PGPR}} = \gamma_{\text{PGPR}2} \cdot G \tag{16}$$

Where γ_{PGPB2} denotes the impact factor of PGPB with respect to the maximum environmental carrying capacity of crops.

Nocturnal bat pollination—unimpeded by abiotic constraints and amplified by extended flight duration and range—significantly enhances crop growth rate; its contribution is denoted r_{Bat} :

$$r_{\text{Bat}} = \gamma_{\text{Bat1}} \cdot C \cdot e^{-\gamma_{\text{Bat2}} \cdot \frac{P_i}{C}}$$
 (17)

Where γ_{Bat1} represents the influence factor of bats on the growth rate of agricultural crops; γ_{Bat2} denotes the ratio influence factor.

With the inclusion of PGPB and bat pollination, the producer dynamics are changed as:

$$r_i = (r_{i0} + r_{\text{PGPB}} + r_{\text{Bat}}) \cdot e^{-\delta t}$$

$$\tag{18}$$

$$K_{i}(t) = (K_{i0} + K_{PGPB}) \cdot \left(1 + \alpha \cdot \sin\left(\frac{\pi}{6}t\right)\right)$$
 (19)

3. Case Analysis

After comprehensive consideration, the Eastern Hubei Yangtze River Plain is selected as the target area for the analysis of agricultural ecosystems [13]. As an important component of the middle and lower reaches of the Yangtze River, this plain has extensive distribution of agricultural land. Certain areas feature a relatively short cultivation history, and the ecosystem structure is comparatively simple. Such ecological conditions are highly compatible with the requirements of the model developed in this study, providing an ideal scenario for its application. This facilitates a deeper exploration of the intrinsic patterns and dynamic changes within agricultural ecosystems.

3.1. Case 1: Fundamental model

In the established model, the simulation is set to begin in the spring following deforestation, with a simulation duration of three years. Furthermore, all pests within the system are classified as primary consumers, while bats and birds are considered secondary consumers.

A range of natural processes and anthropogenic factors are accounted for, thereby delineating six distinct ecosystems according to varying conditions. These ecosystems are defined as follows: A: Original ecosystem, B: Excluding agricultural cultivation, C: Excluding seasonal variations, D: Excluding enrichment effects, E: excluding pesticide use, F: excluding herbicide use.

Experimental Data: To ensure the scientific validity and reliability of the model construction, survey data from Hou Yubai et al. and various relevant online resources are utilized as data sources for selection and calculation to determine the model parameters. Some specific parameters are presented in Table.1. In the table, PC denotes primary consumers, and SC denotes secondary consumers. Meanwhile, Biomass = Density × Weight.

| Parameter | Density | Mean Weight | Max_Biomass | r_i | Initial_Biomass |
|-----------|---------|-------------|-------------|-------|-----------------|
| Crop | 20 | 20 | 400 | 0.2 | 0.1 |
| Weed | 100 | 3 | 300 | 0.4 | 200 |
| PC | 54 | 0.1 | 5.4 | 0.3 | 1 |
| SC | 0.001 | 50 | 0.05 | 0.1 | 0.1 |

Table 1. Empirical Parameters

The interspecific competition and anthropogenic impact parameters were set as follows: competition coefficients between crops and weeds of $d_{ij} = 0.20$ and $d_{ji} = 0.80$; impact coefficients of primary consumers on crops $\gamma_C = 0.10$, of pesticides on primary consumers $\gamma_D = 0.0005$, and of herbicides on weeds $\gamma_P = 0.20$; predation efficiency of secondary consumers on primary consumers $g_i = 0.05$ with predation coefficient $f_{ji} = 0.10$; seasonal fluctuation in carrying capacity $\alpha = 0.05$; accumulation coefficients of harmful substances in producers, primary consumers, and secondary consumers of $\beta = 0.0001$, 0.0002, and 0.001, respectively; and a crop-harvest proportion $p_{\text{harvest}} = 0.80$.

Results Analysis: The actual parameters were input into the established model, followed by plotting the temporal variations in biomass for each population. The resultant changes in the six ecosystems are depicted in Figure 3.

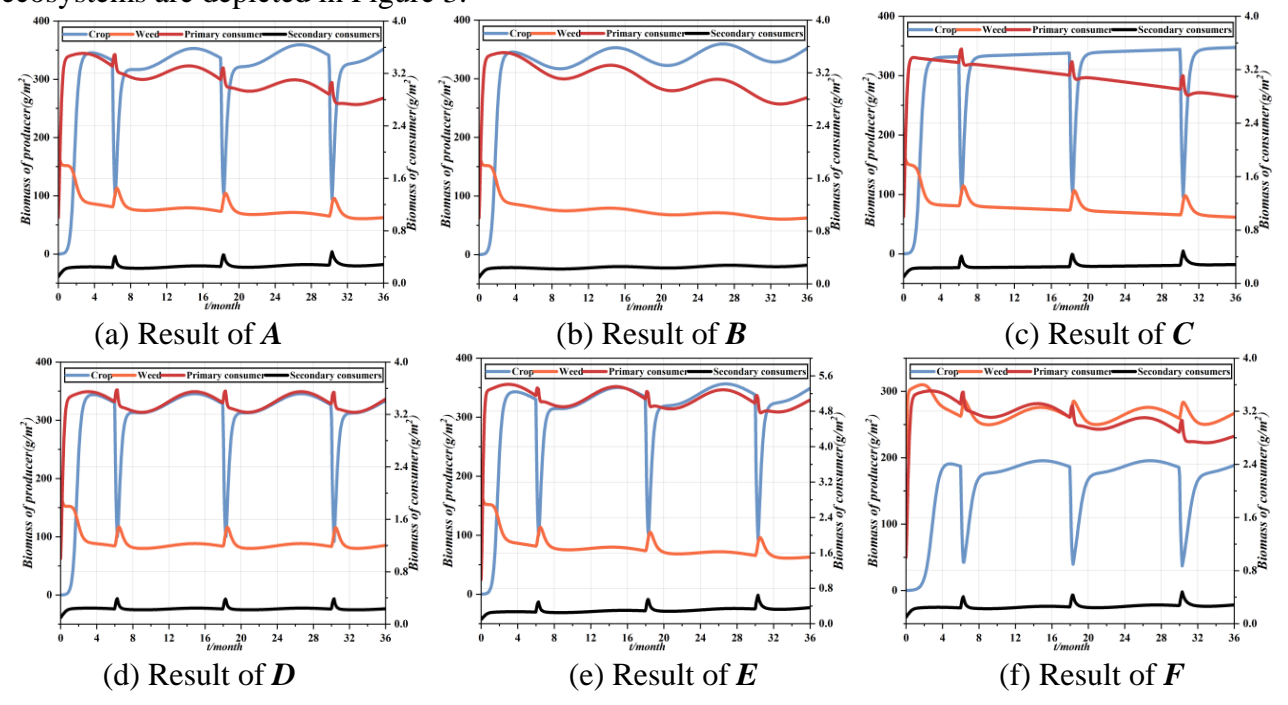


Figure 3. Temporal trajectories of population biomass under varying limiting factors

The study generated six diagrams for ecosystems labeled as *A*, *B*, *C*, *D*, *E*, and *F*. In Figure 3(a), natural and anthropogenic factors jointly drive ecosystem component changes. Without agricultural cultivation and harvesting (Figure 3(b)), crop population fluctuations change, highlighting its key role in ecosystem stability. Excluding seasonal variation (Figure 3(c)), species population fluctuation loses seasonal traits, showing its importance in regulating ecosystem dynamic balance via environmental carrying capacity and growth rates. Removing the enrichment effect (Figure 3(d)) alters primary consumer abundance, indicating its influence on ecosystem stability through biodiversity. Absence of pesticides (Figure 3(e)) and herbicides (Figure 3(f)) changes pest and weed populations, signifying chemical agents' regulatory role and potential ecosystem risks.

3.2. Case 2: Reemergence of Species

During the second year of succession, two consumer species were added: mice (secondary consumers) and snakes (tertiary consumers), with bats representing both bats and birds by functional equivalence. Mice exploit crops and pests with an intrinsic growth rate $r_m = 0.10$ and a crop-damage coefficient $q_r = 0.001$. Snakes grow at $r_s = 0.05$, predate on mice with efficiency $a_m = 0.20$, and incur a self-growth cost $c_m = 0.50$. Incorporation of these parameters into the enhanced model produces the producer and consumer biomass trajectories shown in Figure 4.

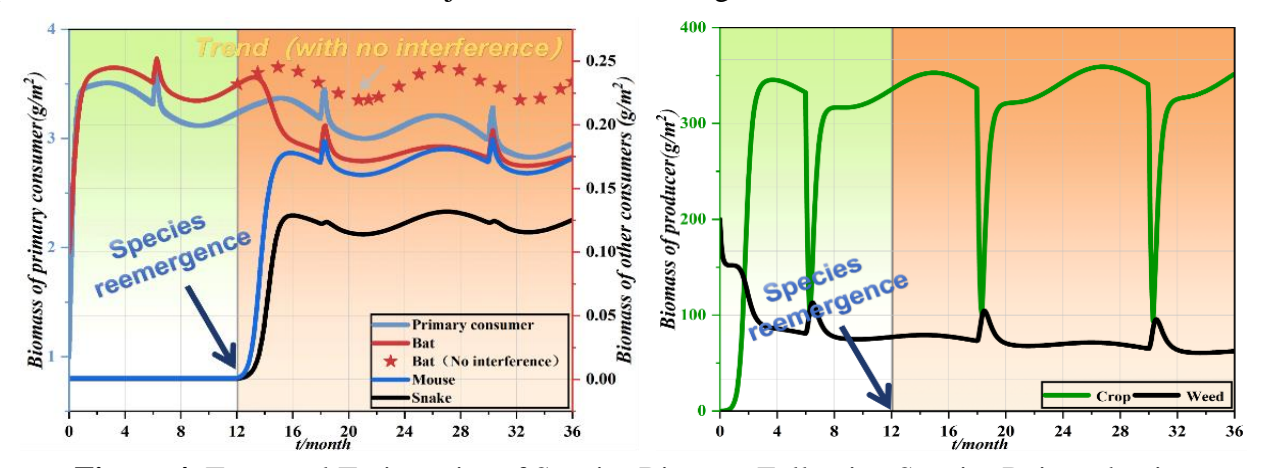


Figure 4. Temporal Trajectories of Species Biomass Following Species Reintroduction

As is discernible from Figure 4, subsequent to the introduction of mice and snakes in the second year of the study, their biomass initially exhibited an exponential growth tendency and subsequently leveled off gradually. The biomass of mice surpassed that of snakes and approximated the quantity of bats. Within the original ecosystem framework, the introduction of mice and snakes exerted a substantial influence on the biomass of bats, impeding the growth of bats, whilst having a marginal effect on producers and other consumers.

3.3. Case 3: Decomposer Incorporation and Pollination Role

Based on Case 2, Plant Growth-Promoting Bacteria (PGPB) and bat pollination efficacy were incorporated into the model. The parameters γ_{PGPB2} , γ_{Bat1} and γ_{Bat2} were set to 0.05, 0.20 and 300, respectively, and the maximum environmental capacity of PGPB was fixed at $2 \times 10^7 \, \text{CFU/g}$. Simulations were carried out for four scenarios: the original model; the model including only decomposers; the model including only bat pollination; and the model in which both decomposers and bat pollination were combined. The resulting trajectories of ecosystem succession are shown in Figure 5.

As discernible from Figure 5, subsequent to the incorporation of PGPB, the biomass of crops exhibits a progressive increment in tandem with the augmentation of the PGPB population. When the PGPB population nears its maximum accommodating capacity, the crop biomass levels off. Throughout this progression, the growth rate of crops remains virtually unaltered in comparison to that of the original ecosystem.

Upon the introduction of bat pollination, the upward trajectory of crop biomass becomes more pronounced than that of the original ecosystem, albeit the terminal stabilized biomass is approximately equivalent to that of the original one. When both PGPB and bat pollination are concurrently integrated, the crop biomass not only manifests a swifter growth rate but also attains a significantly elevated stabilized biomass relative to the original ecosystem.

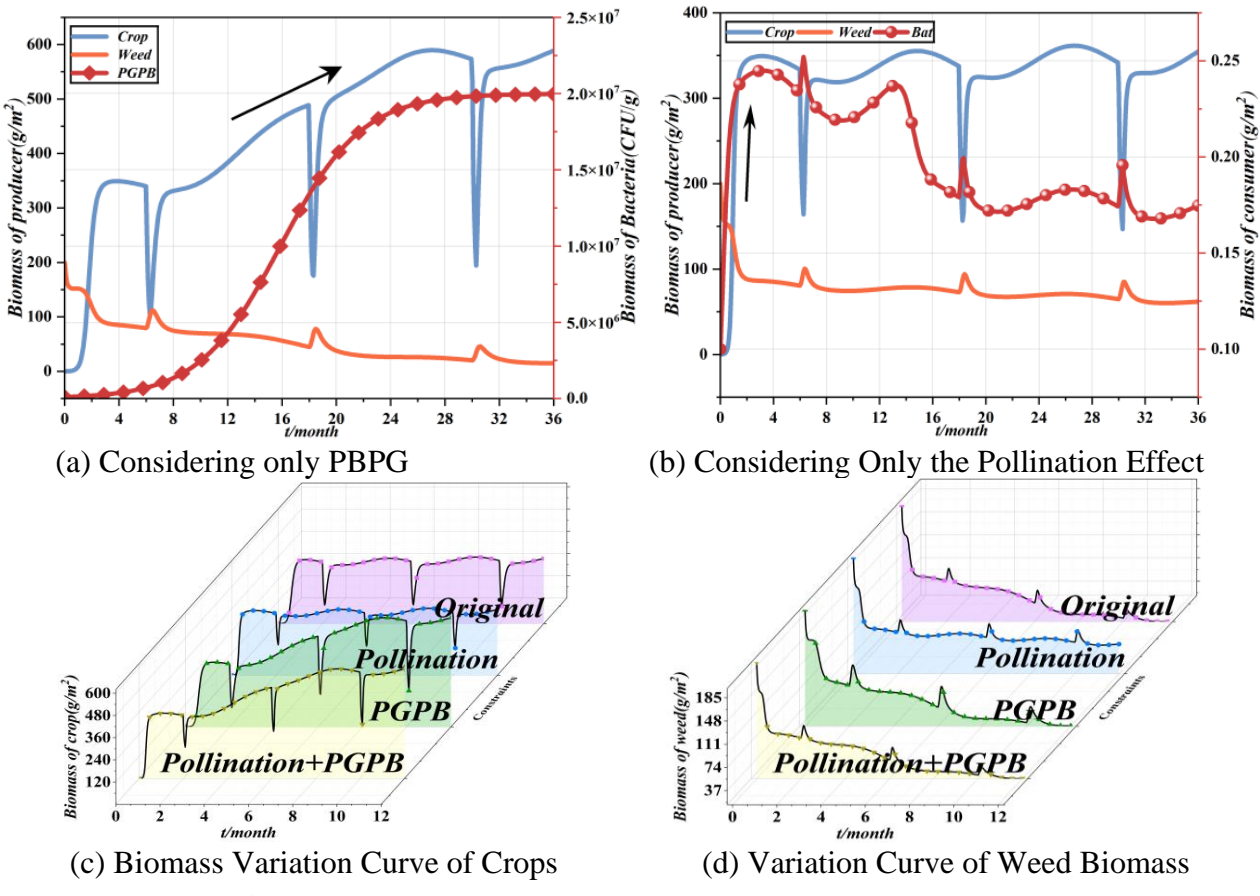


Figure 5. The Impact of Pollination and PBPG on Ecosystems

4. Conclusion

This study establishes a dynamic DM model to simulate evolutionary processes in agricultural ecosystems, aiming to clarify mechanisms of ecosystem stability. Three case studies empirically validate the model's applicability in predicting trophic interactions, species introduction impacts, and biological interventions.

Case 1 systematically analyzes the agricultural ecosystem in the Eastern Hubei River Plain across six hypothetical scenarios, revealing how biotic-abiotic interactions regulate ecosystem stability. The findings validate the theoretical model's practical applicability, offering empirical guidance for refining agricultural management strategies to enhance ecosystem resilience.

Simulation of case2 analysis identifies snakes as apex tertiary consumers inducing trophic cascades: predation on bats reduces their biomass and dominance, while mice exhibit biomass synchronization due to shared resource competition. Primary consumers (pests) maintain stability via dietary diversity, and producer biomass remains unaltered by top-down trophic dynamics.

Evaluation of case3 demonstrates that Plant Growth-Promoting Bacteria (PGPB) primarily enhance resistance stability by increasing crop biomass and resource utilization efficiency, with secondary improvements in resilience via functional redundancy. Bat pollination, conversely, predominantly strengthens resilience stability, enabling rapid recovery of plant biomass after perturbations such as extreme weather or pest infestations.

Future research should integrate dynamic DM models with spatial heterogeneity and climate-change scenarios to reveal how extreme weather, terrain, and soil variability affect agro-ecosystem stability. It should also incorporate socioeconomic and policy factors for eco-economic assessments, extend models to pathogen–microbe interactions for biocontrol insights, and improve calibration through long-term field trials and remote sensing to close the model–data–decision loop.

References

- [1] Hofmeister Kathryn L., Feitl Gwen, Tackett Kaylee, et al. Land-use effects on soil organic matter and related soil properties in a mixed agricultural-forest landscape of central Wisconsin, USA [J]. Soil Science Society of America Journal, 2025, 89 (1).
- [2] Druckenbrod Daniel, Norton Dean. Tree rings, forest composition, and LiDAR reveal historical forests and past agricultural land use at George Washington's Mount Vernon [J]. Progress in Physical Geography Earth and Environment, 2025, 49 (1-2): 101 119.
- [3] Wu Xian, Deane David C., Xing Hua, et al. Structure and functions of soil microbial communities and tree composition are more closely associated with keystone microbes than rare microbes in a subtropical forest [J]. Journal of Plant Ecology, 2025, 18 (1).
- [4] Marton Lorinc, Hangos Katalin M., Magyar Attila. Migration-connected networks of Lotka–Volterra and quasi-polynomial systems: modeling and decentralized control [J]. Nonlinear Dynamics, 2025, 113 (9): 10577 10596.
- [5] Ma, Chenfei, Zhang, Xiaofeng, Yuan, Rong. Dynamic analysis of a stochastic regime-switching Lotka-Volterra competitive system with distributed delays and Ornstein-Uhlenbeck process [J]. Chaos Solitons & Fractals, 2025, 190.
- [6] Amarathunga DC, Parry H, Grundy J, et al. A predator-prey population dynamics simulation for biological control of Franklinville occidentalis (Western Flower Thrips) by Orius laevigatus in strawberry plants [J]. Biological Control, 2024, 188: 105409.
- [7] Tang JJ, Jiang LW, Wang X, et al. Salt-tolerant plant growth-promoting bacteria enhanced the growth and alleviated salt toxicity to maize by increasing K⁺/Na⁺ homeostasis [J]. International Journal of Environmental Science and Technology, 2025, 22 (8): 6637 6650.
- [8] Zhang Can, Kong Xiangzhen, Xue Bin, et al. Double-edged effects of anthropogenic activities on lake ecological dynamics in northern China: Evidence from paleolimnology and ecosystem modelling [J]. Freshwater Biology, 2023, 68 (6): 940 955.
- [9] Fonte A, Garcera C, Chueca P. Spray volume adjustment for pesticide applications against aphids in citrus: Validation of CitrusVol tool [J]. Crop Protection, 2025, 194: 107187.
- [10] Bell L, Lignou S, Wagstaff C. High Glucosinolate Content in Rocket Leaves (Diplotaxis tenuifolia and Eruca sativa) after Multiple Harvests Is Associated with Increased Bitterness, Pungency, and Reduced Consumer Liking [J]. Foods, 2020, 9 (12): 1799.
- [11] Tilhou N, Kucek LK, Moore V, et al. Seed size has a major impact on fall seedling vigor in the cover crop hairy vetch (Vicia villosa Roth) [J]. Crop Science, 2025, 65 (1).
- [12] Pacada IG, Cantila AY. Assessing yield variation in rice varietal mixtures (VarMix®) and single varieties across 12 environments using AMMI analysis [J]. SciEnggJ, 2024, 17 (2): 286 294.
- [13] Hou Y. Rural eco-environmental issues [J]. Rural Eco-Environment, 1997, 13 (2): 33 36, 52.